

## APPENDIX V

### PREDICTION OF ELECTRON SPECTRA IN HIGH ENERGY ELECTRON-PROTON SCATTERING

A pair of computer programs have been completed which will predict the electron spectra expected when electrons of primary energies up to 20 BeV are scattered from protons. The first program, known as the Interpolation Routine (abbreviated IR) computes the e-p elastic scattering cross sections, the e-p inelastic cross sections that produce an isobar nucleon state, and those inelastic cross sections for excitations of the recoiling system greater than 500 MeV. For a specified laboratory scattering angle, primary electron energy, and a specified maximum energy loss, the IR program generates cross sections over the range required by the second program (known as the Backward Program or BP) which employs the IR output as its main input. The BP introduces radiative effects into the spectra furnished by IR. The analytic forms of the cross sections employed in IR are the most recent ones found from fits to the CEA electron-proton scattering results (for the elastic events), from the most recent analysis by Hand of the Panofsky-Allton experiment (for the electroproduction of pions through the isobar state) and from a combination of the CEA bubble chamber studies of very inelastic ( $\gamma, p$ ) reactions for gamma energies to 6 BeV and the proton form factors.

In this appendix, the important equations we employ and the method by which the radiative effects are introduced will be briefly discussed.

#### A. THE INTERPOLATION ROUTINE

We consider the spectrum of electrons  $\sigma(E_i, E_f, \theta) \equiv d^2\sigma/d\Omega dE_f$  for scattering of electrons of primary energy  $E_i = E_{\text{initial}}$ , at laboratory angle  $\theta$ , to a final energy  $E_f = E_{\text{final}}$ . If when the maximum value of  $E_{\text{initial}}$  is  $E_0$  and the minimum final electron energy is  $E_{\text{final}}^{\text{min}} = E_0 - K_0$  we must, in order to introduce radiative effects consistently, know the cross sections over a triangular region as indicated in Figure 1. We divide the kinematic domain into three regions and call them Case I, II and III. Case I is for e-p elastic scattering, Case II is for excitation of the (3, 3) resonance (assuming the state has zero width), and Case III is for excitation energy greater than 0.5 BeV in the rest frame of the recoiling system.

For Case I, we use the Rosenbluth formula and the CEA pole-fit form factors to calculate the cross sections.

For Case II, the cross section is given by

$$\left(\frac{d\sigma}{d\Omega}\right)_{ep \rightarrow eN_{33}^*} = \left(\frac{d\sigma}{d\Omega}\right)_{\text{Mott}} \left(\frac{\alpha}{4\pi^2 e^4}\right) \text{STG}_{\text{MV}}^2(q^2)$$

where

$$q^2 = 4 E_i E_f \sin^2 \frac{\theta}{2}$$

$$S = A_0 K \frac{E_i}{E_f} \frac{1}{1 + \frac{2E_i}{M} \sin^2 \frac{\theta}{2}}$$

$$T = \left[ \frac{q^2}{q^2 + (E_i - E_f)^2} + 2 \tan^2 \frac{\theta}{2} \right]$$

$$K = E_i - E_f - \frac{q^2}{2M}$$

and the constant  $A_0$  is determined by the normalization condition

$$\int \left(\frac{d\sigma_\gamma(K)}{dK}\right)_{\gamma p \rightarrow N_{33}^*} dK = A_0 \int \delta(K' - K) dK'$$

where the (3, 3) resonance has been taken to be a  $\delta$ -function of energy  $K$ .

For Case III, the cross section is given by

$$\frac{d^2\sigma}{d\Omega dE_f} = \left(\frac{d\sigma}{d\Omega}\right)_{\text{Mott}} \frac{\alpha}{4\pi^2 e^4} K \frac{E_i}{E_f} \left[ \frac{2q^2}{q^2 + (E_i - E_f)^2} + 2 \tan^2 \frac{\theta}{2} \right] (100 \mu\text{b}) G_{\text{MV}}^2(q^2)$$

Here, for lack of information, we have arbitrarily assumed that the longitudinal and the transverse photons contribute equally, and that the photoproduction cross section to be constant and equal to  $100 \mu\text{b}$ .

Employing the above expressions, the IR compute all the entries in a triangle of given dimensions. Out of voluminous output, one spectrum is shown in Figure 2.

It should be pointed out that spectra as observed at the higher resolutions to be employed at SLAC will appear much different near the elastic peaks than in our plots as our results give the yields correctly for the much coarser resolution employed in the calculation. In particular the SLAC spectrometers will, in all circumstances, resolve elastic scattering from isobar production, and the peaks, being much narrower, will be correspondingly higher.

#### B. THE BACKWARD PROGRAM

The backward program has been derived from a previously existing program that unfolds out of observed electron spectra the corrected yields. It is the correction program run (logically) backward, hence the name. It takes account of real photon emission in the target before and after scattering, as well as the real and virtual photon corrections to the scattering process itself.

The cross sections we employ increase so rapidly as the primary electron energy decreases that portions of the spectra for large electron energy losses are modified substantially. Our results can be used to identify the regions of the spectra which are usefully sensitive to the important cross sections and are not dominated by events from radiative degradation of higher energy processes. Figure 3 shows two spectra with spectrometer resolution  $\Delta E = 50$  MeV. They illustrate how the program deals with distributing the elastic scattering yield between mesh points in kinematic variables, and also indicate the radiative effects on the resolved elastic and (3,3) resonance scattering. The dashed lines in the figure, marked as zero target radiator length, include only the real and virtual photons corrections to the scattering process itself, whereas the solid lines include the real photon emission both before and after scattering in the 0.03 r.l. thick target.

We have also used Yang's exponential form factor,  $e^{-|q|/0.6}$ , to calculate the elastic peak and associated radiative tail at high  $q^2$  beyond the existing experimental limit. The difference in the predicted spectra by using the CEA pole-fit and the Yang's form factors are fairly pronounced at  $E'_0 = 20$  BeV and  $\theta = 15^\circ$ , as shown in Fig. 4. The difference becomes larger at higher  $q^2$ .

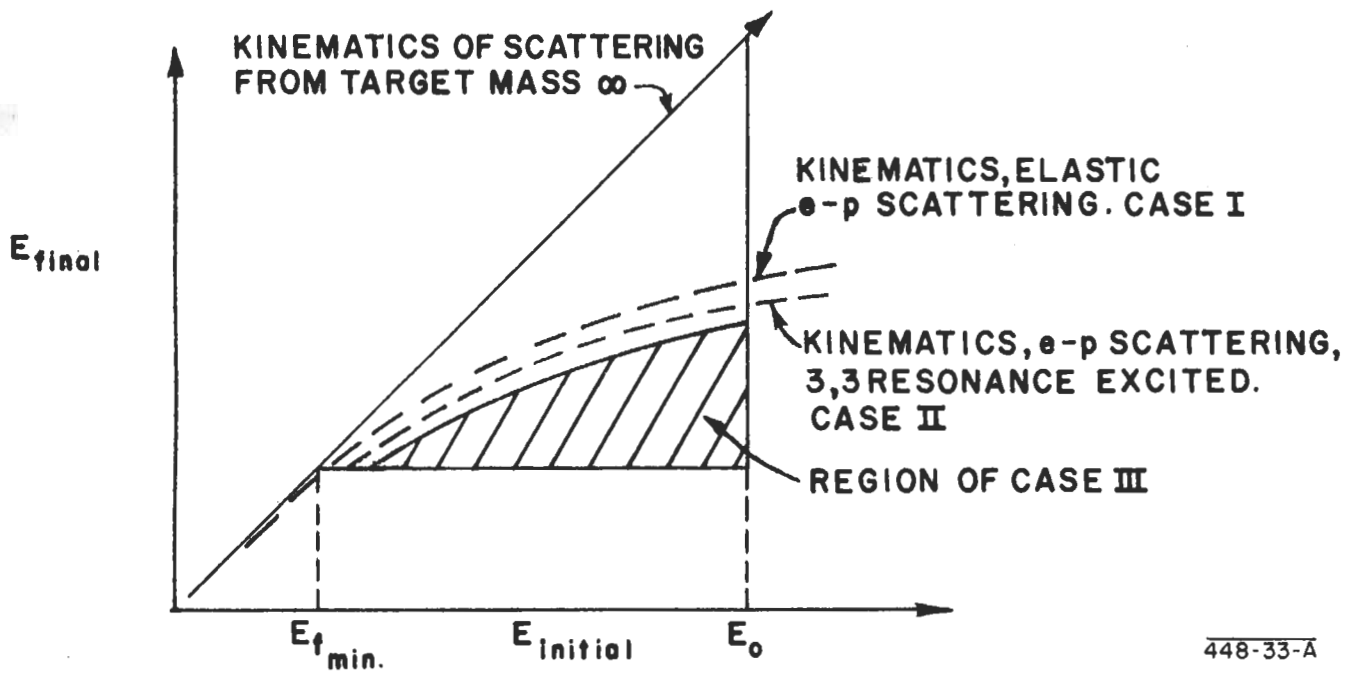
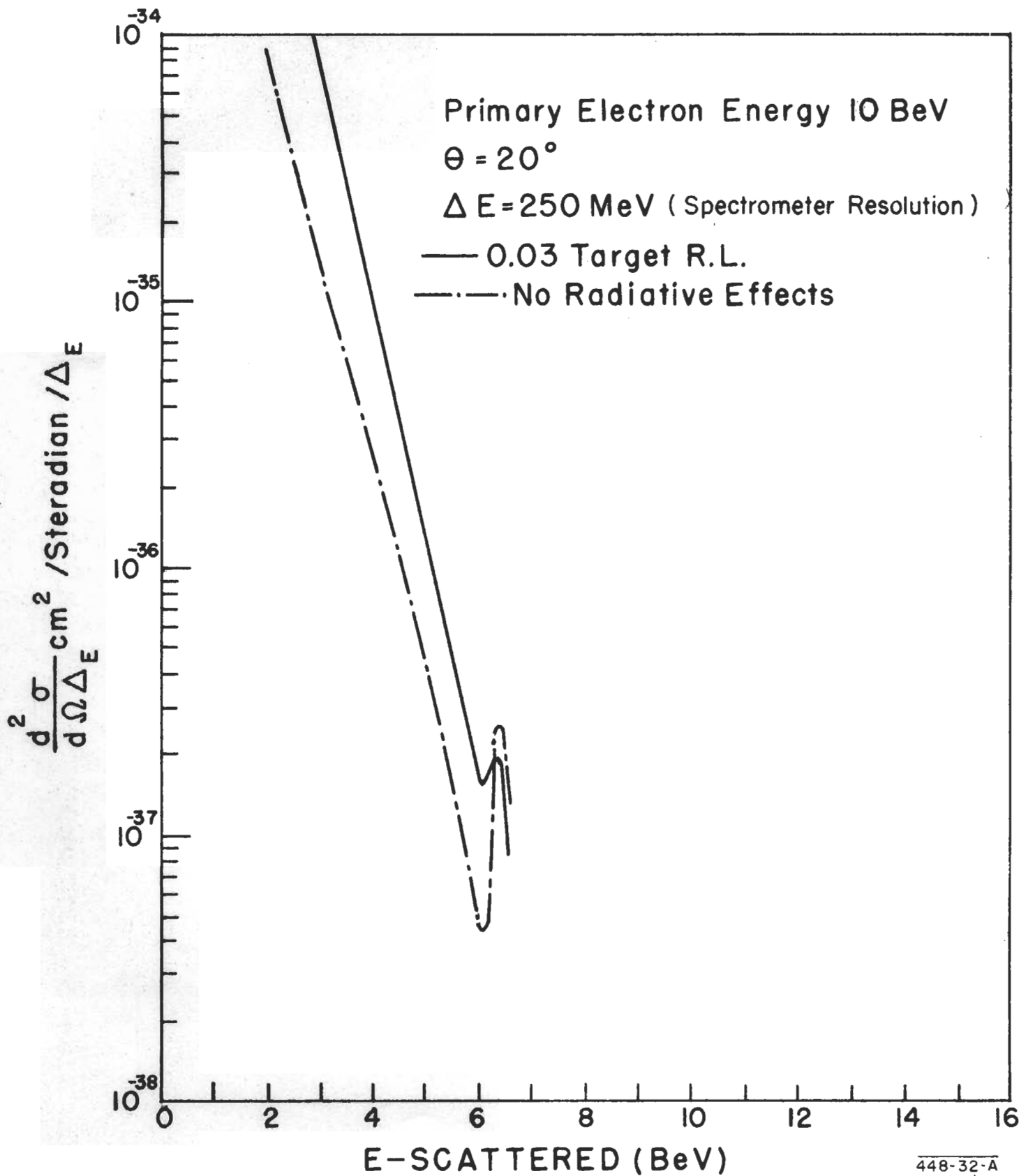


Figure 1



448-32-A

Fig. 2

*(Handwritten signature)*

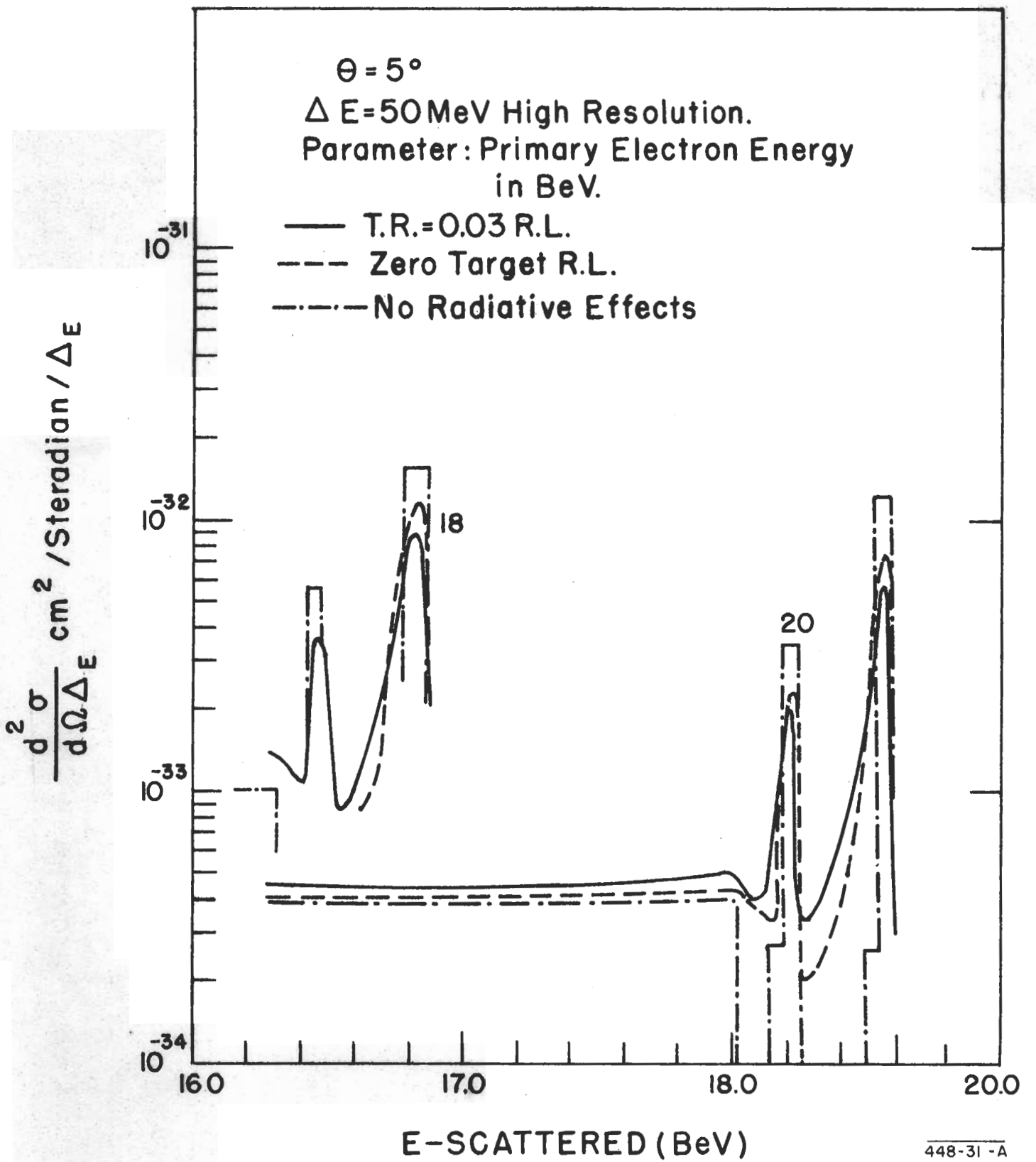


Fig. 3

APP 5

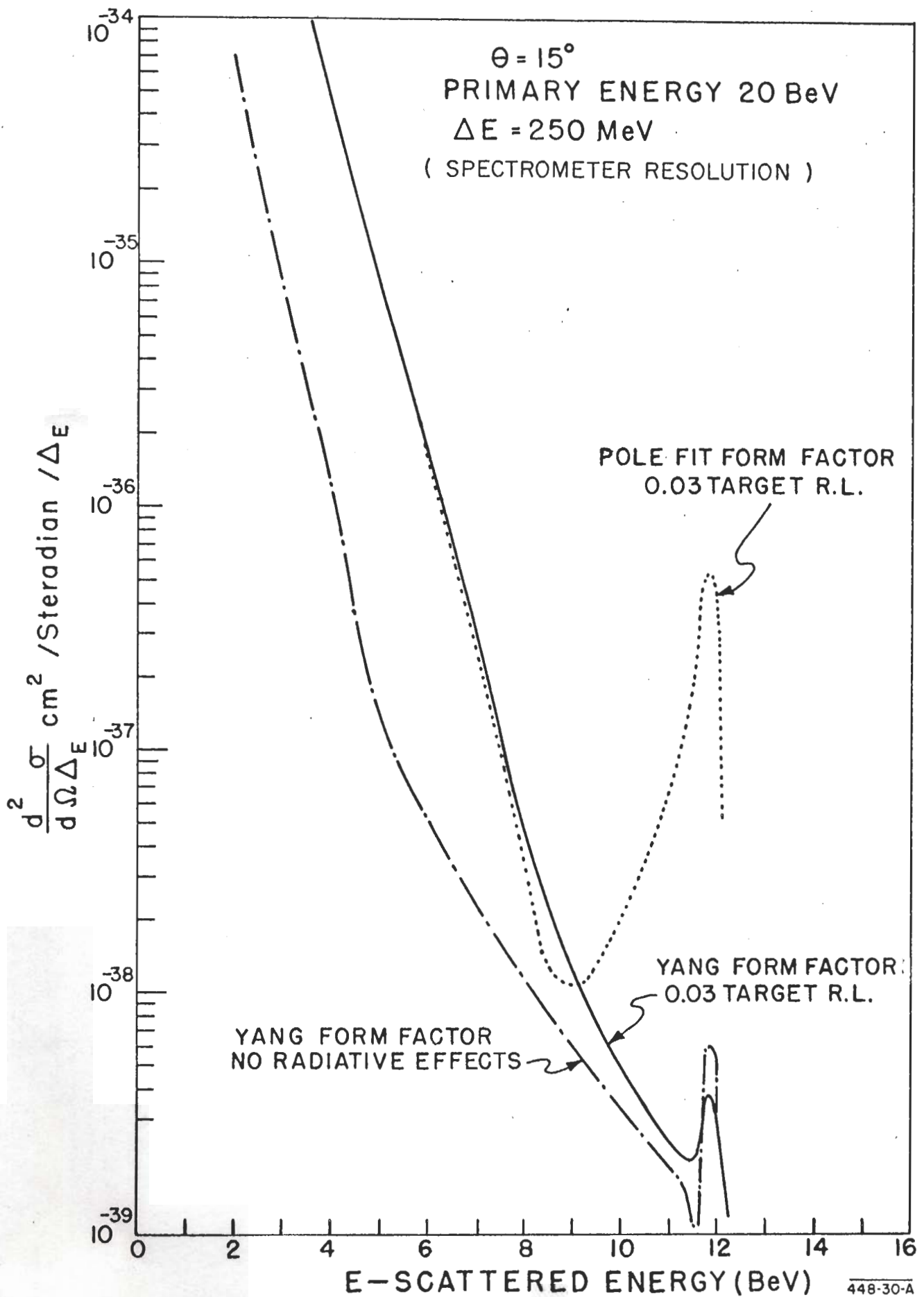


Fig. 4